



SEDIMENT BUDGET OF LIDO OF PELLESTRINA (VENICE)

Written by Marcello Di Risio

Under the supervision of Giorgio Bellotti and Leopoldo Franco

Table of contents:

1. Introduction.....	3
2. Protection structures system.....	3
3. Methodologies of sediment budget.....	4
4. Surveys.....	5
5. Volumes and areas computation.....	6
6. Hypothesis to explain the volumes evolution.....	14
7. Conclusions and further work.....	22

List of figures:

Figure 1: Plan view of Lido of Pellestrina (all the cells).....	3
Figure 2: Plan view of Lido of Pellestrina (only the first eleven cells).....	3
Figure 3: Plan view of the protection structures system.....	4
Figure 4: Section in the middle of a cell.....	4
Figure 5: Sections position in a cell.....	5
Figure 6: Sand volumes variations with respect to initial conditions (ΔV_0) at survey II for the 10 cells.....	8
Figure 7: Sand volumes variations with respect to initial conditions (ΔV_0) at survey III for the 10 cells.....	8
Figure 8: Sand volumes variations with respect to initial conditions (ΔV_0) at survey IV for the 10 cells.....	9
Figure 9: Sand volumes variations with respect to initial conditions (ΔV_0) at survey V for the 10 cells.....	9
Figure 10: Sand volumes variations with respect to initial conditions (ΔV_0) at survey VI for the 10 cells.....	10
Figure 11: Sand volumes variations with respect to initial conditions (ΔV_0) for cell 1.....	10
Figure 12: Sand volumes variations with respect to initial conditions (ΔV_0) for cell 2.....	10
Figure 13: Sand volumes variations with respect to initial conditions (ΔV_0) for cell 3.....	11
Figure 14: Sand volumes variations with respect to initial conditions (ΔV_0) for cell 4.....	11
Figure 15: Sand volumes variations with respect to initial conditions (ΔV_0) for cell 5.....	11
Figure 16: Sand volumes variations with respect to initial conditions (ΔV_0) for cell 6.....	12
Figure 17: Sand volumes variations with respect to initial conditions (ΔV_0) for cell 7.....	12
Figure 18: Sand volumes variations with respect to initial conditions (ΔV_0) for cell 8.....	12
Figure 19: Sand volumes variations with respect to initial conditions (ΔV_0) for cell 9.....	13
Figure 20: Sand volumes variations with respect to initial conditions (ΔV_0) for cell 10.....	13
Figure 21: Comparison between nourishment dates (black points) and surveys date (gray lines) for each cell (x axis values).....	14
Figure 22: Wave climate (mean wave height for each month).....	14
Figure 23: Shoreline variations with respect to initial conditions at survey II.....	15
Figure 24: Shoreline variations with respect to initial conditions at survey III.....	15
Figure 25: Shoreline variations with respect to initial conditions at survey IV.....	15



Figure 26: Shoreline variations with respect to initial conditions at survey V 16

Figure 27: Shoreline variations with respect to initial conditions at survey VI..... 16

Figure 28: Shoreline variations with respect to initial conditions at cell 1 for all six surveys 16

Figure 29: Shoreline variations with respect to initial conditions at cell 2 for all six surveys 17

Figure 30: Shoreline variations with respect to initial conditions at cell 3 for all six surveys 17

Figure 31: Shoreline variations with respect to initial conditions at cell 4 for all six surveys 17

Figure 32: Shoreline variations with respect to initial conditions at cell 5 for all six surveys 18

Figure 33: Shoreline variations with respect to initial conditions at cell 6 for all six surveys 18

Figure 34: Shoreline variations with respect to initial conditions at cell 7 for all six surveys 18

Figure 35: Shoreline variations with respect to initial conditions at cell 8 for all six surveys 19

Figure 36: Shoreline variations with respect to initial conditions at cell 9 for all six surveys 19

Figure 37: Shoreline variations with respect to initial conditions at cell 10 for all six surveys 19

Figure 38: Wave direction distribution along time (mean month direction)20

Figure 39: Sketch of the zones definition 20

Figure 40: Areas evolution of the different zones for the section close to the South groyne with respect to the initial conditions 21

Figure 41: Areas evolution of the different zones for the section in the middle of cell 9 with respect to the initial conditions..... 21

Figure 42: Areas evolution of the different zones for the section close to the North groyne with respect to the initial conditions 22

Figure 43: Volume evolution For each cell 23

List of tables:

Table I: Beach surveys chronology 5

Table II: Section definition (coordinates of start point and azimuth in centesimal angle respect to North direction)..... 6

Table III: Beach sand volumes data in Pellestrina cells..... 7

1. Introduction

The present document is aimed to investigate effects of the system structures defence built at Lido of Pellestrina through a budget of sediments. In the following the protection structures system is briefly described, methodologies of sediment budget are presented and surveys are illustrated. The computation regards only the first eleven cells, because there are enough surveys only for the south part of the beach (see. fig. 1) from cell 0 to cell 10 wich are the older.

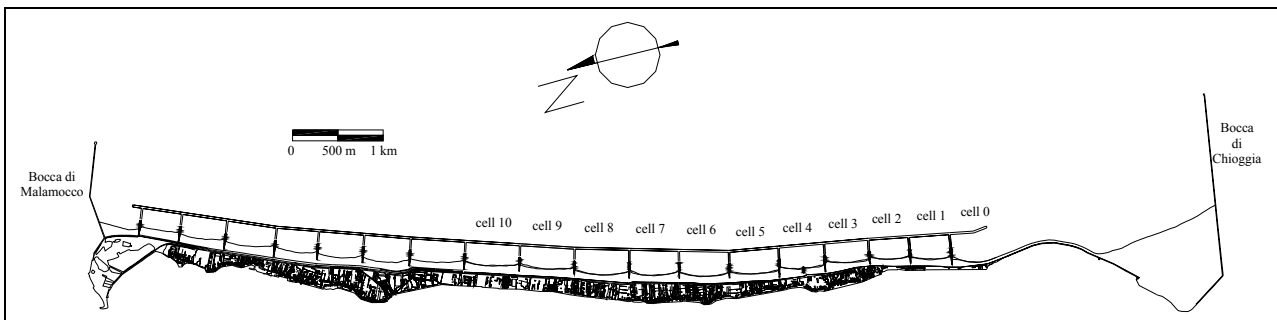


Figure 1: Plan view of Lido of Pellestrina (all the cells)

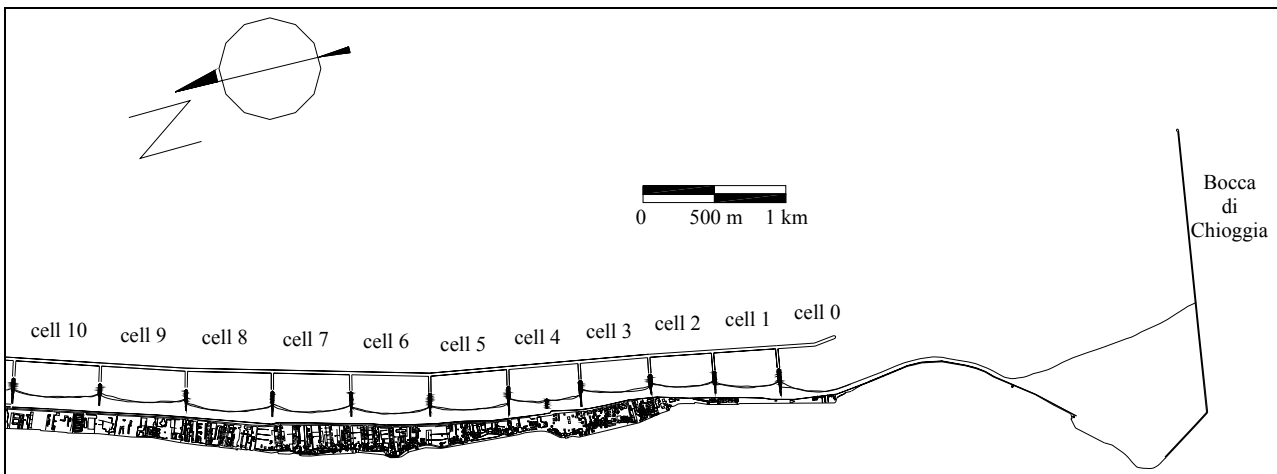


Figure 2: Plan view of Lido of Pellestrina (only the first eleven cells)

2. Protection structures system

To defend the Lido of Pellestrina, since 1995 a system of partially submerged groynes and a submerged breakwater was built with beach nourishment (about 4.000.000 m³ of sand dredged from offshore and pumped onto the new beach). The groynes are joined to the submerged longitudinal breakwater. The result is a system of partially closed cells (see fig. 3). Groynes are about 150÷210 m long with the crest at about +2.2÷2.7 m above the mean water level and for their first 100 m they are on the beach. These groynes are joined to the submerged breakwater through a submerged part with the crest positioned at -1.5 m below the mean water level. Finally the submerged breakwater has not any gap, its crest is positioned at 1.5 m below the mean water level and width of about 14 m, its position is about 300 m from shoreline (see fig. 4).

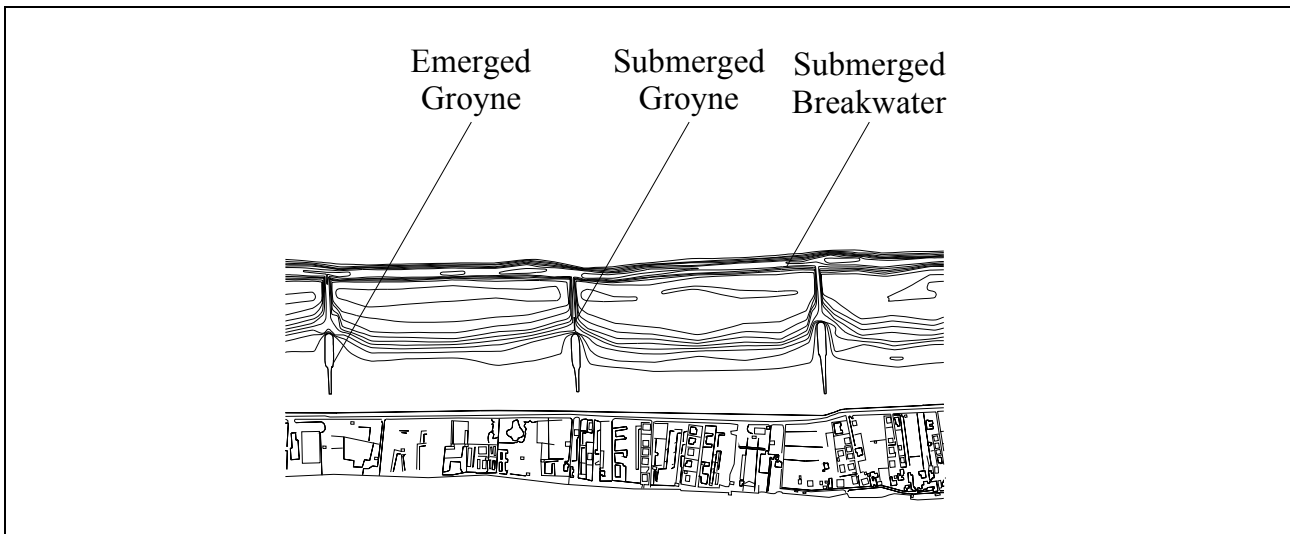


Figure 3: Plan view of the protection structures system

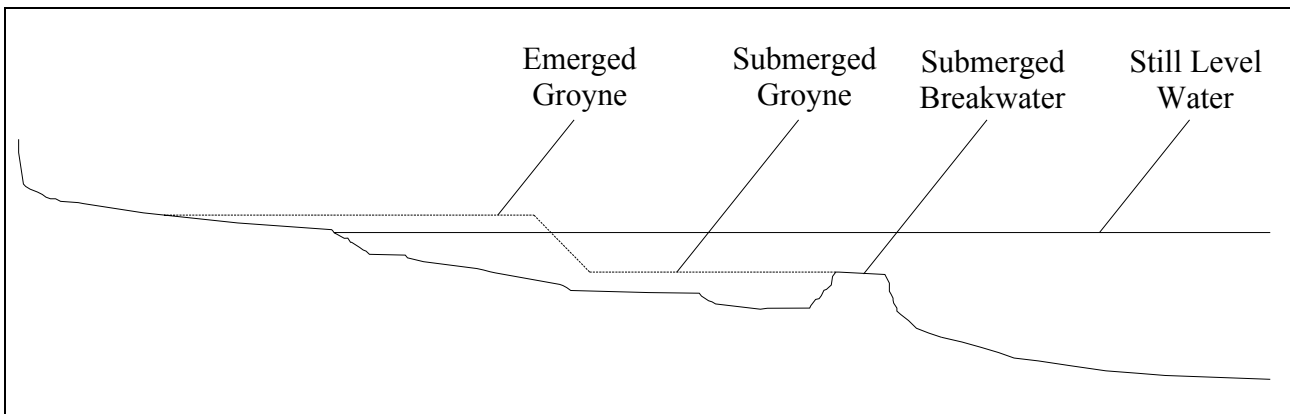


Figure 4: Section in the middle of a cell

3. Methodologies of sediment budget

This work was carried out through computing of volumes and areas to understand preliminarily the sediment transport effects in the first eleven cells of the Lido of Pellestrina. With these computations it is possible to estimate the sand quantity loss or gain but it is not possible to assert where it went, in the loss case, or where it came from, in the gain case.

The results obtained with this methodology are interesting in order to understand the protection structures system behaviour with respect to the trapping of sand pumped onto the beach in the nourishment operations. The same results are not interesting to understand the direction of the longshore sediment transport ratio or the transversal transport losses.

In order to operate in this last aspect another methodology of sediment budget exists. It consists in a simple application of the principle of conservation of mass to the littoral sediments: *the time rate of change of sand within the system is dependent upon the rate at which sand is brought into the system versus the rate at which sand leaves the system* (from “Beach processes and sedimentation” by Paul D. Komar). To do this it is needed to evaluate the importance of several sediment sources and losses to the nearshore zone (longshore transport, river transport, sea cliff erosion, biogenous transport, wind transport, etc.). It is clear that this last estimation is very difficult in most real cases.



For the Lido of Pellestrina (all the cells) it is possible to consider the nearshore system as a closed one and it is needed to evaluate only the longshore and cross-shore transport (the wind, biogenous and similar contribution can be omitted). Further work is to utilize a one-line model to estimate these transport ratios and understand where the sand goes and not only if it is gone away (see “Conclusions and further works” section).

4. Surveys

The results of the computation presented here are based on six surveys performed in order to monitor the site. These surveys (see tab. I) are carried out by boat along sections with

Survey	Date	
	Month	Year
I	October	1997
II	July	1998
III	March	1999
IV	September	1999
V	June	2000
VI	December	2000

Table I: Beach surveys chronology

known locations in the Gauss-Boaga coordinates (see tab. II). The surveys precision is about ± 10 cm, but it is possible to consider a Gaussian distribution of the errors and therefore the surveys data are assumed to be quite good. All surveys were corrected for tidal fluctuation (± 0.50 m) and referred to mean sea level.

All the surveys give the profile of the beach along the monitoring sections from the murazzo into the beach to a short distance from the submerged breakwater in its offshore side (see tab. II). Profiles were utilized to areas computing as described in the following section (“Volumes and areas computation”). It is necessary to pay attention to the sections position: for each cell three cross sections are carried out, one in the middle of it and two close to the groynes (see fig. 5).



Figure 5: Sections position in a cell



Cell	Section	Section Definition		
		N	E	Azimut
		[m]	[m]	[gone]
0	10	5014982.86	2308071.95	103.522
	14	5015224.25	2308106.09	109.719
1	15	5015290.09	2308122.19	110.452
	18	5015453.84	2308171.97	110.621
	21	5015617.09	2308211.95	110.542
2	22	5015687.39	2308227.8	110.482
	25	5015851.64	2308265.37	110.482
	28	5016010.53	2308309.7	110.482
3	29	5016082.29	2308319.19	111.738
	32	5016253.2	2308333.53	111.738
	35	5016455.34	2308340.51	111.738
4	36	5016519.69	2308348.2	109.479
	39	5016703.99	2308370.22	109.479
	42	5016855.99	2308385	109.479
5	43	5016971.55	2308398.16	109.534
	46	5017172.85	2308432.65	109.534
	50	5017397.52	2308470.61	109.534
6	51	5017471.04	2308484.85	116.358
	54	5017691.68	2308531.86	116.358
	57	5017893.66	2308590.05	116.358
7	58	5017954.09	2308604.86	114.906
	61	5018159.45	2308657.63	114.906
	64	5018371.14	2308710.93	114.906
8	65	5018433.15	2308717.27	114.998
	68	5018663.99	2308792.99	114.998
	71	5018891.44	2308867.59	114.998
9	72	5018954.99	2308889.03	115
	75	5019171.51	2308956.12	115
	78	5019409.72	2309026.09	115
10	79	5019480.62	2309048.05	117.736
	82	5019708.33	2309118.13	117.736
	85	5019937.41	2309185.56	117.736

Table II: Section definition (coordinates of start point and azimuth in centesimal angle respect to North direction)

5. Volumes and areas computation

For all surveys the areal computation was carried out considering areas between a segment at a fixed depth (here at 7 m below the mean water level) and the lines that represent the cross-shore profile. Then volumes were computed considering the “*influence area*” of each section. For each cell of width c , the influence area of the central section is $c'/2$ width and the one of the lateral sections are $c'/4$, where c' is the distance between the two sections close to the groynes (hence $c \approx c'$).

Table III contains the values of beach sand volumes obtained with this methodology.



Cells	Survey	t	V	ΔV	ΔV_0	ΔV_r
		month	[m ³]	[m ³]	[m ³]	[%]
1	I	0	644024	0	0	0.00
	II	9	643988	-37	-37	-0.01
	III	17	641099	-2889	-2926	-0.73
	IV	23	636389	-4709	-7635	-1.91
	V	32	638465	2075	-5559	-1.39
	VI	38	631581	-6884	-12443	-3.11
2	I	0	583966	0	0	0.00
	II	9	578337	-5629	-5629	-1.41
	III	17	535207	-43130	-48759	-12.19
	IV	23	586986	51779	3020	0.76
	V	32	573739	-13247	-10227	-2.56
	VI	38	559103	-14636	-24863	-6.22
3	I	0	717303	0	0	0.00
	II	9	737534	20232	20232	5.06
	III	17	695473	-42061	-21830	-5.46
	IV	23	723695	28222	6392	1.60
	V	32	731200	7505	13897	3.47
	VI	38	713139	-18061	-4164	-1.04
4	I	0	697697	0	0	0.00
	II	9	714705	17008	17008	4.25
	III	17	712245	-2460	14548	3.64
	IV	23	691892	-20352	-5804	-1.45
	V	32	710085	18193	12388	3.10
	VI	38	706169	-3916	8472	2.12
5	I	0	873801	0	0	0.00
	II	9	883906	10104	10104	2.53
	III	17	849301	-34605	-24500	-6.13
	IV	23	875719	26418	1917	0.48
	V	32	890030	14312	16229	4.06
	VI	38	879271	-10759	5470	1.37
6	I	0	774107	0	0	0.00
	II	9	789216	15109	15109	3.78
	III	17	781789	-7427	7682	1.92
	IV	23	773019	-8770	-1089	-0.27
	V	32	783485	10466	9378	2.34
	VI	38	777677	-5808	3569	0.89
7	I	0	823201	0	0	0.00
	II	9	826039	2838	2838	0.71
	III	17	802793	-23246	-20408	-5.10
	IV	23	819224	16431	-3977	-0.99
	V	32	818421	-803	-4780	-1.20
	VI	38	810745	-7676	-12456	-3.11
8	I	0	850823	0	0	0.00
	II	9	886571	35748	35748	8.94
	III	17	868201	-18370	17378	4.34
	IV	23	868025	-176	17202	4.30
	V	32	890737	22712	39914	9.98
	VI	38	876042	-14696	25219	6.30
9	I	0	841988	0	0	0.00
	II	9	876888	34900	34900	8.73
	III	17	901692	24804	59704	14.93
	IV	23	854079	-47614	12091	3.02
	V	32	904552	50474	62564	15.64
	VI	38	896243	-8310	54255	13.56
10	I	0	886085	0	0	0.00
	II	9	926769	40684	40684	10.17
	III	17	946562	19792	60477	15.12
	IV	23	918924	-27638	32839	8.21
	V	32	909474	-9449	23389	5.85
	VI	38	912963	3489	26878	6.72

Table III: Beach sand volumes data in Pellestrina cells



In the third column (t) a temporal coordinate was defined with the zero coincident with the survey of the first month. The fourth column (V) contains the computed volumes. The fifth column (ΔV) contains the volumes variation with respect to the previous survey and the sixth one (ΔV_0) contains the volumes variation with respect to the first survey (it describes the variation with respect to the initial conditions). The last column (ΔV_r) contains the relative volumes percentage variations normalized with the cell nourishment volume (400.000 m^3).

Analysis of these data is possible with aid of graphic charts. The target is to understand the trend of sand volumes variation in space (from cell 1 to cell 10) and in time (from survey I to survey VI). In order to do the following graphs are presented

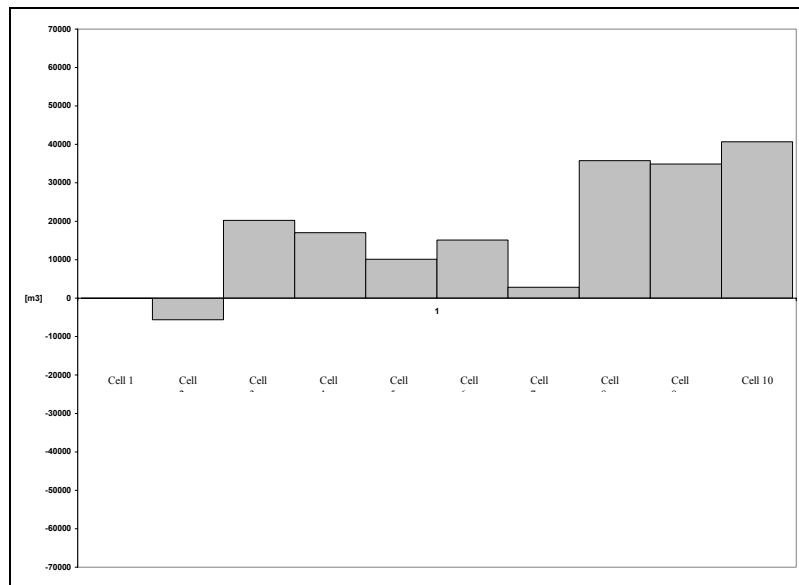


Figure 6: Sand volumes variations with respect to initial conditions (ΔV_0) at survey II for the 10 cells

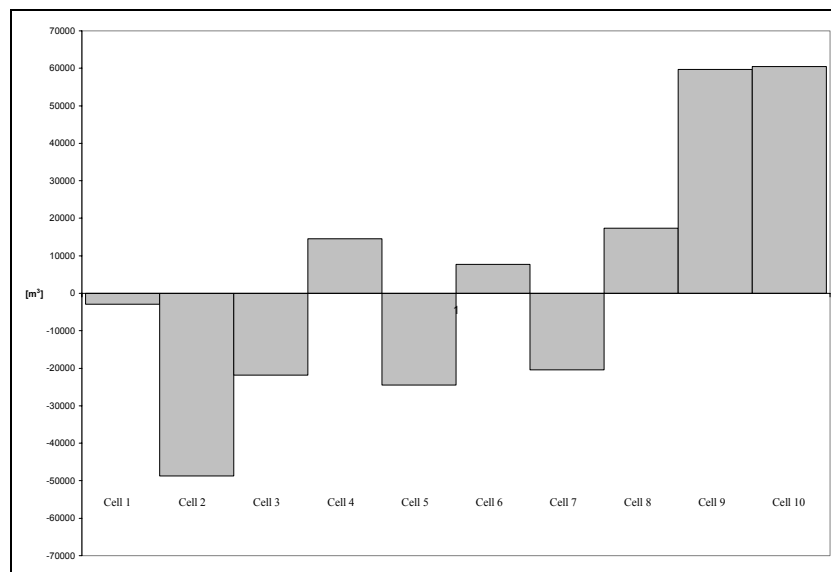


Figure 7: Sand volumes variations with respect to initial conditions (ΔV_0) at survey III for the 10 cells

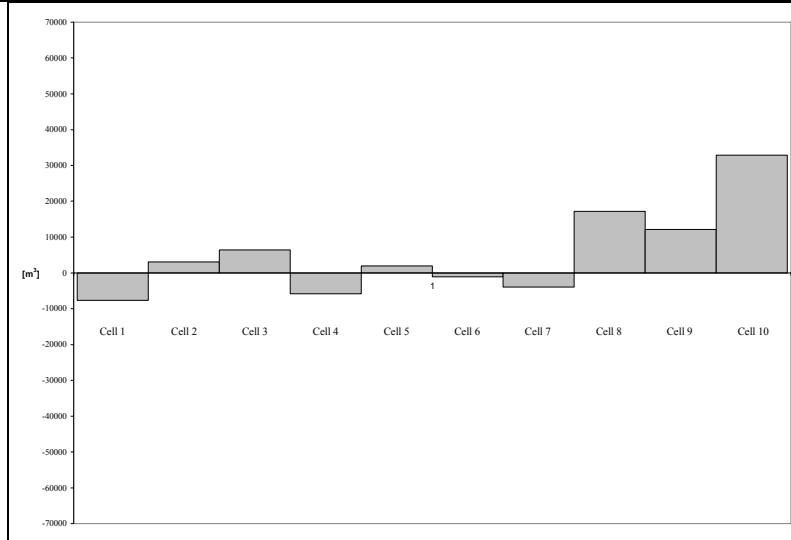


Figure 8: Sand volumes variations with respect to initial conditions (ΔV_0) at survey IV for the 10 cells

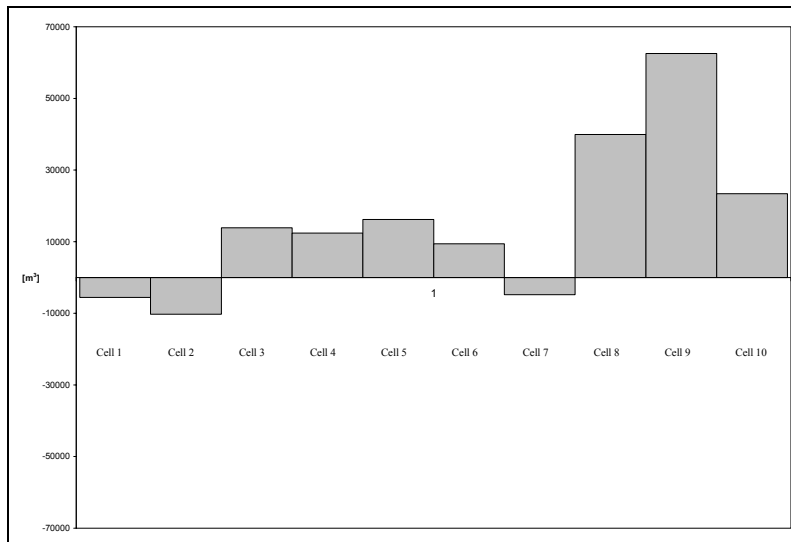


Figure 9: Sand volumes variations with respect to initial conditions (ΔV_0) at survey V for the 10 cells

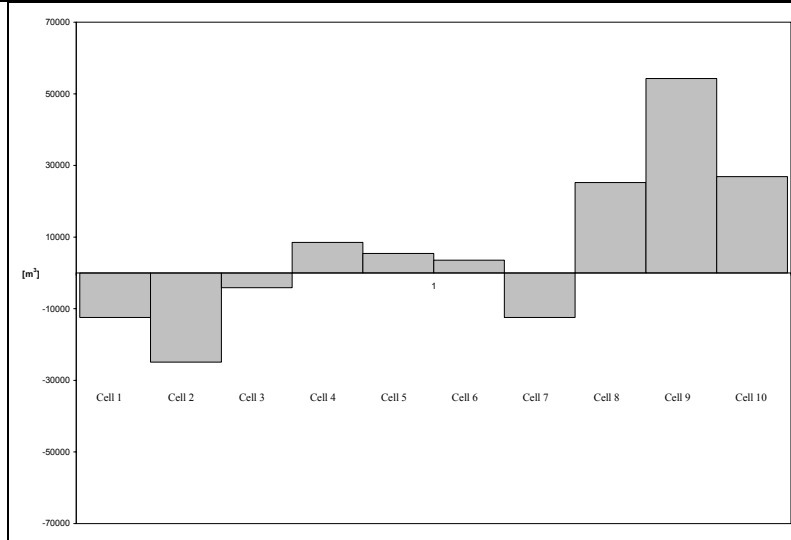


Figure 10: Sand volumes variations with respect to initial conditions (ΔV_0) at survey VI for the 10 cells

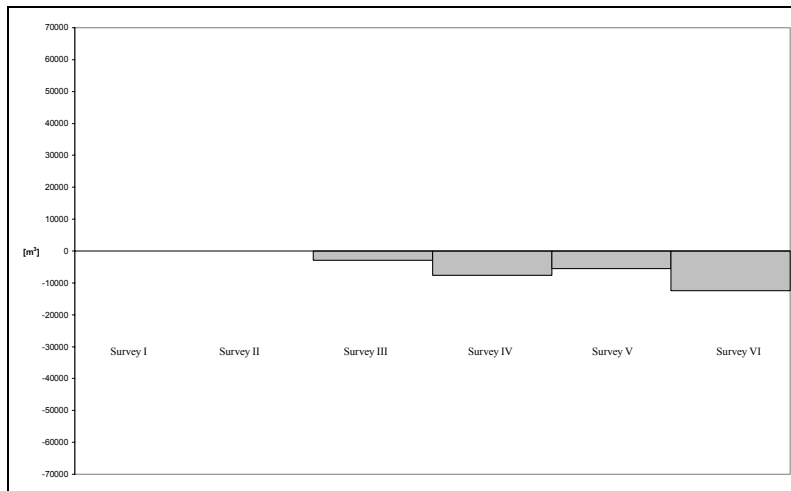


Figure 11: Sand volumes variations with respect to initial conditions (ΔV_0) for cell 1

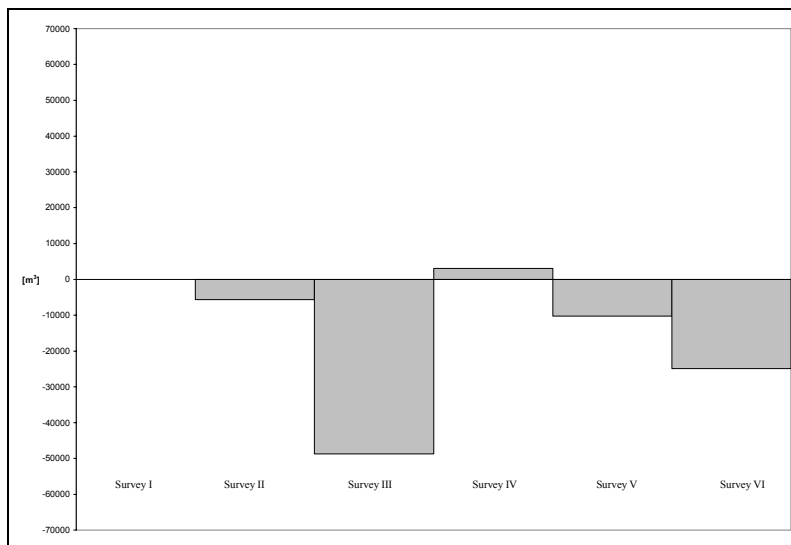


Figure 12: Sand volumes variations with respect to initial conditions (ΔV_0) for cell 2

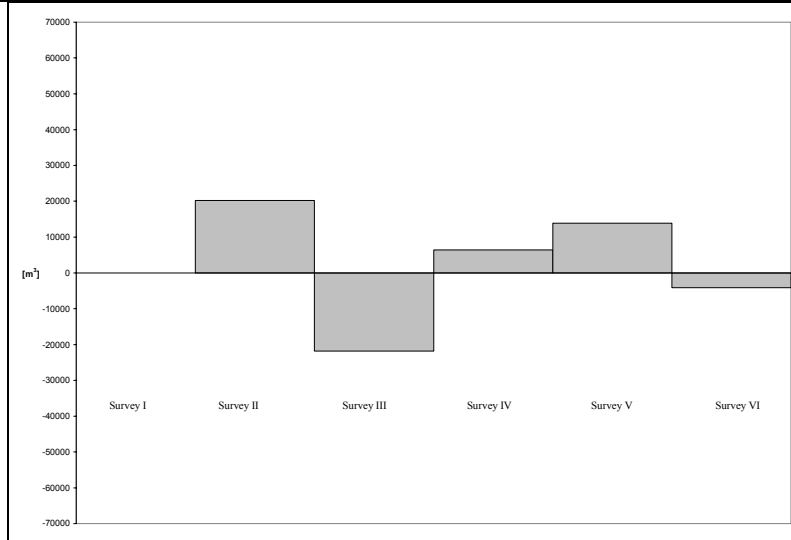


Figure 13: Sand volumes variations with respect to initial conditions (ΔV_0) for cell 3

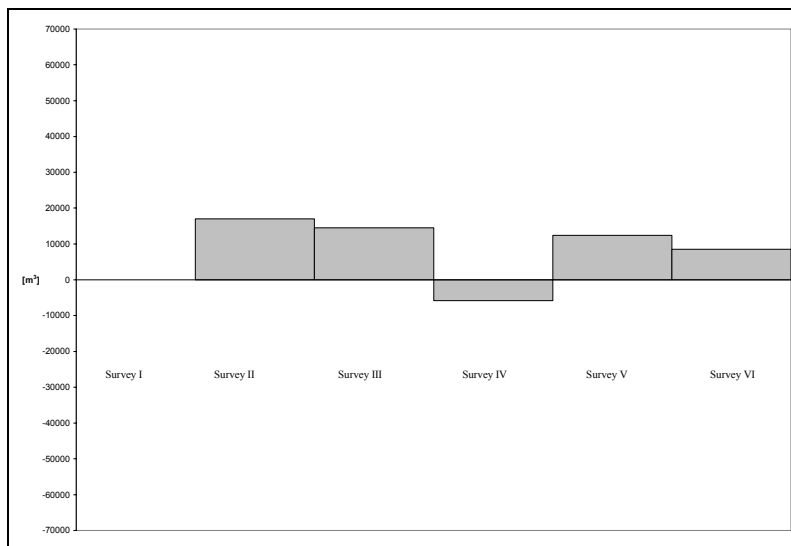


Figure 14: Sand volumes variations with respect to initial conditions (ΔV_0) for cell 4

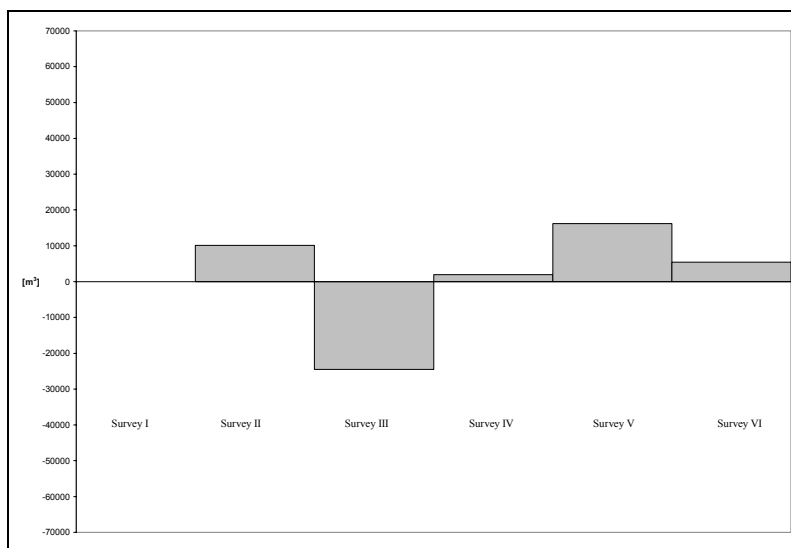


Figure 15: Sand volumes variations with respect to initial conditions (ΔV_0) for cell 5

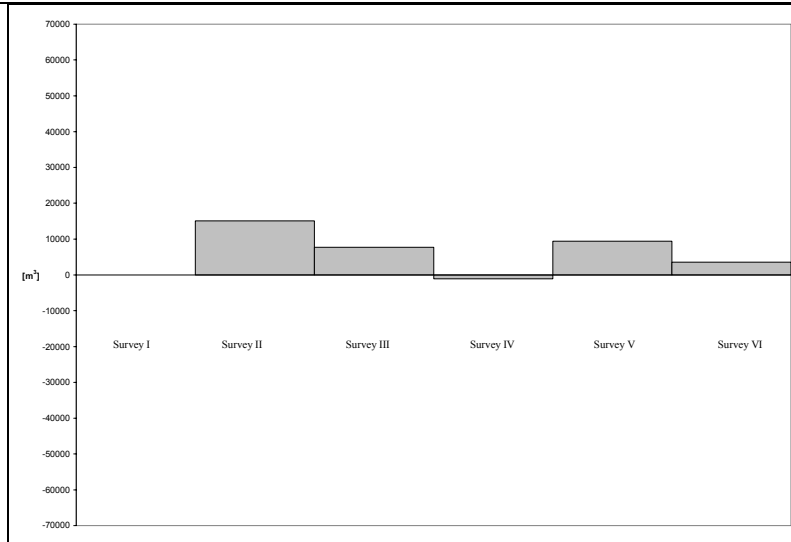


Figure 16: Sand volumes variations with respect to initial conditions (ΔV_0) for cell 6

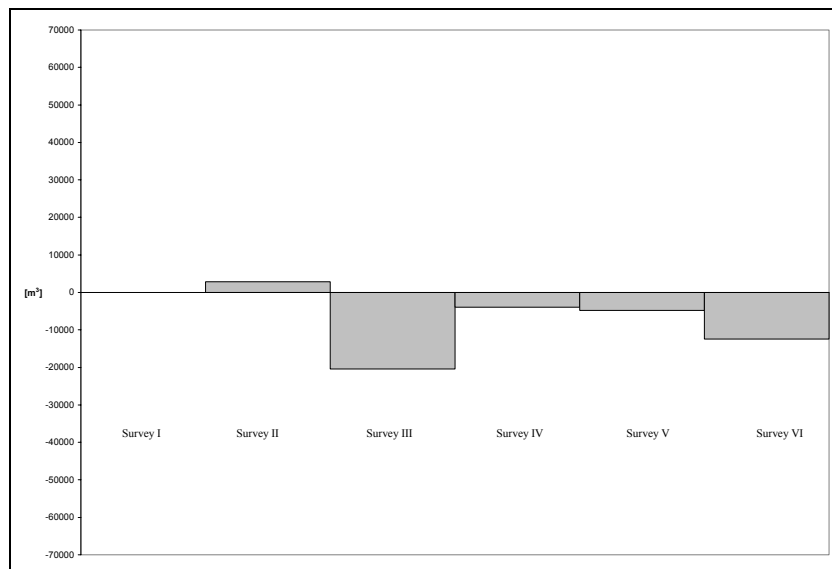


Figure 17: Sand volumes variations with respect to initial conditions (ΔV_0) for cell 7

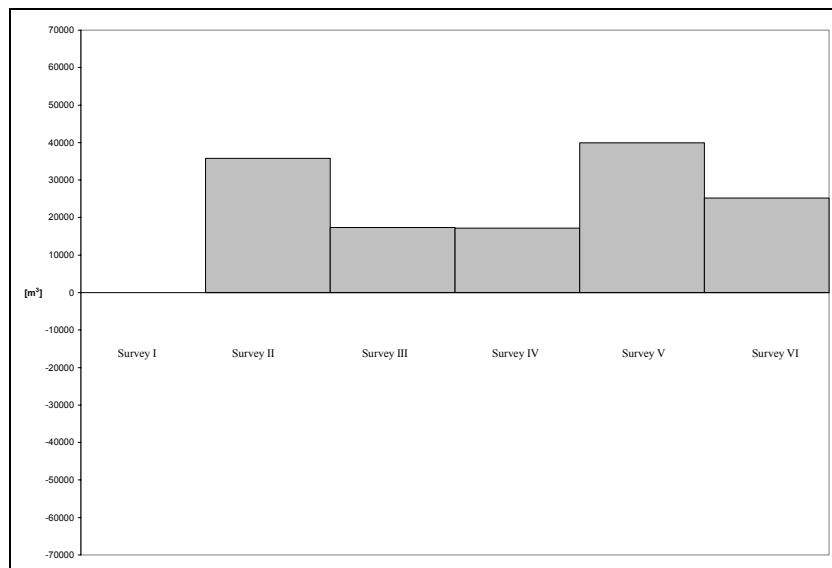


Figure 18: Sand volumes variations with respect to initial conditions (ΔV_0) for cell 8

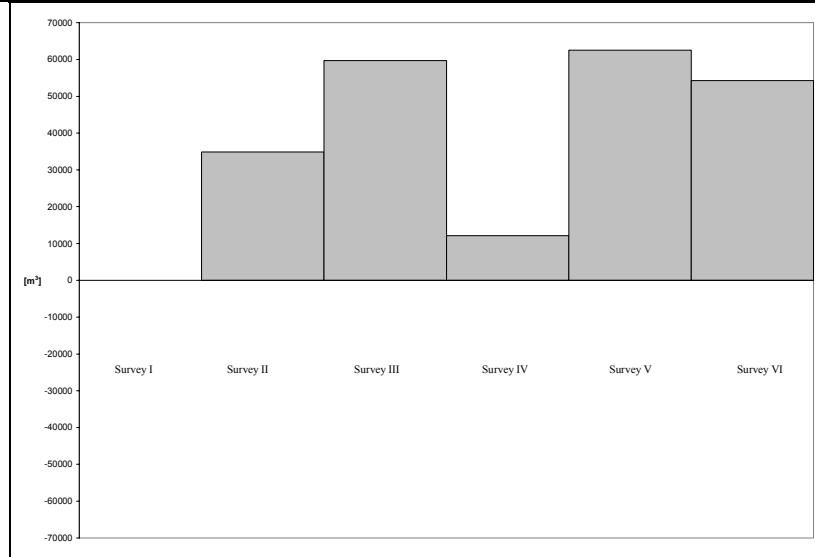


Figure 19: Sand volumes variations with respect to initial conditions (ΔV_0) for cell 9

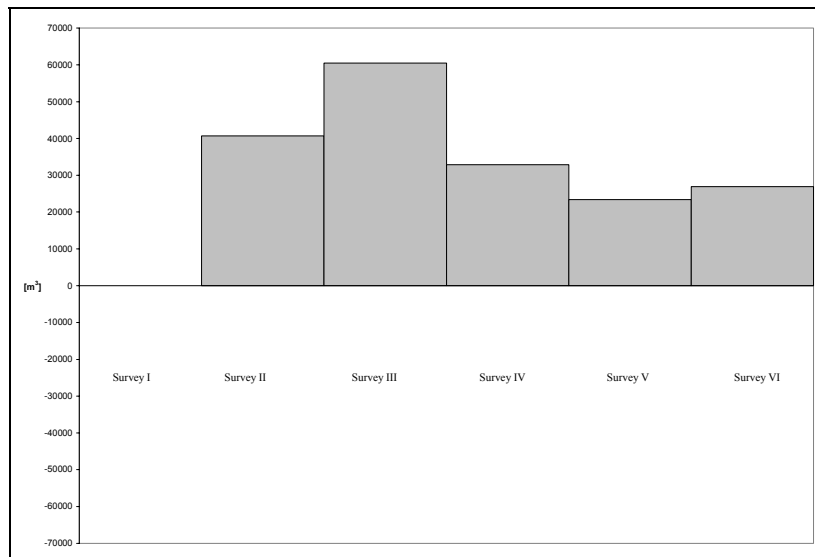


Figure 20: Sand volumes variations with respect to initial conditions (ΔV_0) for cell 10

From the analysis of the spatial evolution (see fig. 6-7-8-9-10) it is clearly observable an evident difference between the first cells and the last three. This distribution of the volumes variation with respect to initial condition can be explained by the dates of the nourishment (May 1997 for these cells). The cells located close to North (cells 8, 9 and 10) are the youngest ones and reshaping phenomena are more important than in the first ones (see fig. 21).

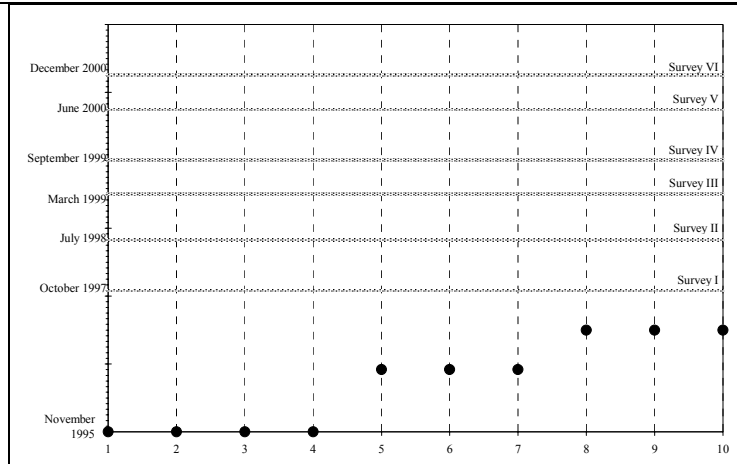


Figure 21: Comparison between nourishment dates (black points) and surveys date (gray lines) for each cell (x axis values)

The temporal evolution for each cell (see fig. 11-12-13-14-15-16-17-18-19-20) can be explained by analysing to the wave climate (see fig. 22) for which, i.e., it is possible to explain the loss of sand of the first cells computed for the survey III, because it follows a severe winter season.

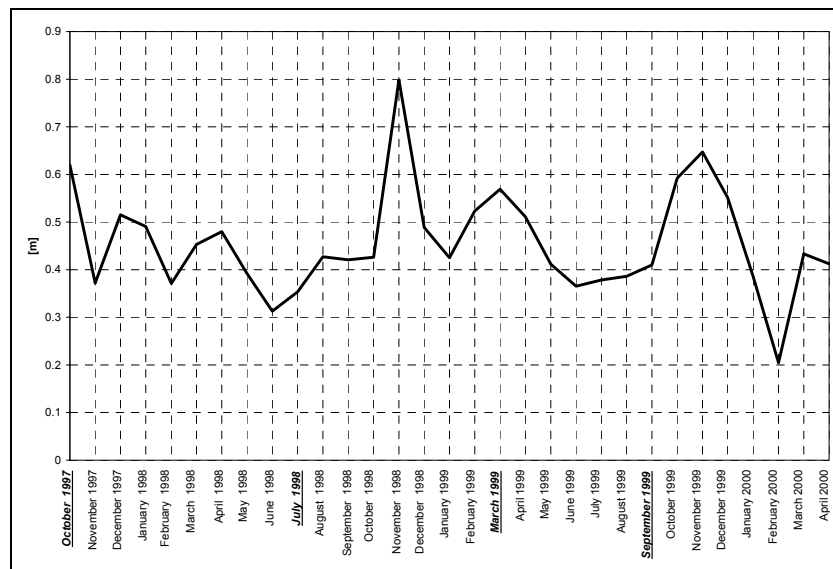


Figure 22: Wave climate (mean wave height for each month)

6. Hypothesis to explain the volumes evolution

At this point of the analysis we can explain the volume evolution. To do this it is possible to analyse the areas distribution along a section. Volumes data can be supported by other information such as the evolution of shoreline position and evolution of the single section.

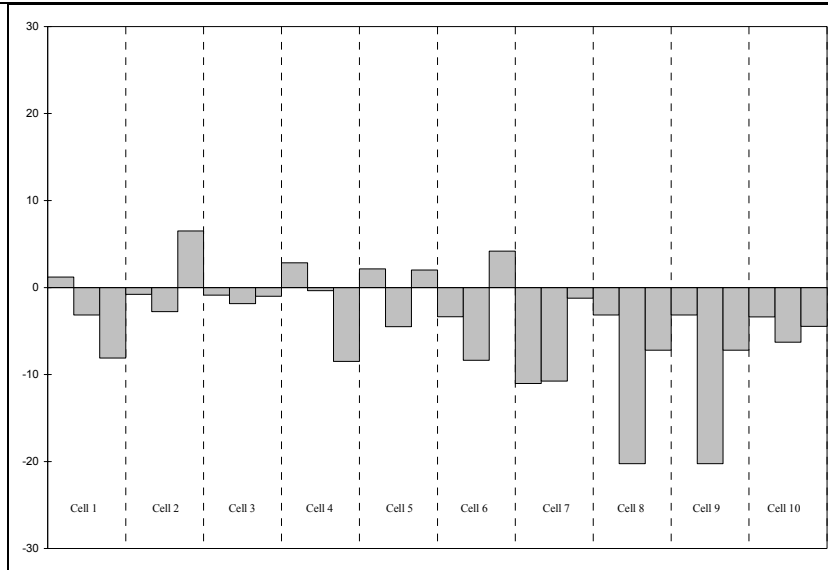


Figure 23: Shoreline variations with respect to initial conditions at survey II

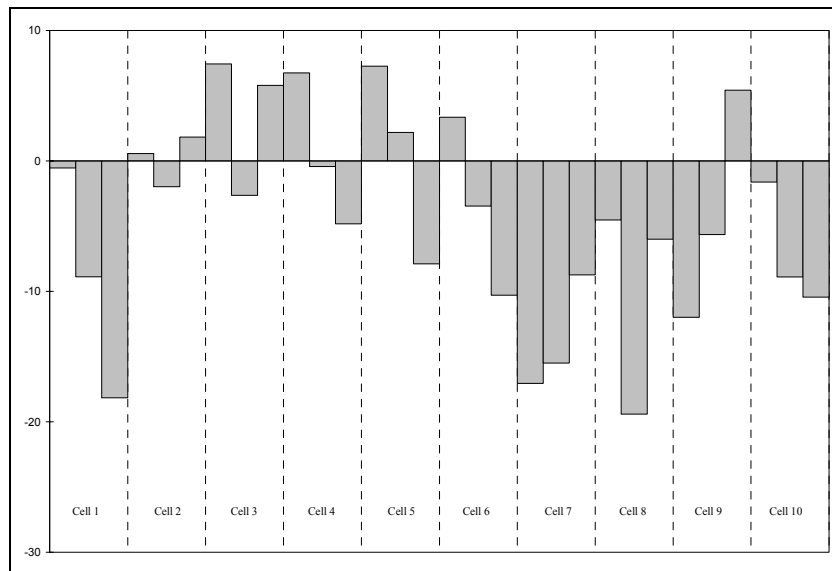


Figure 24: Shoreline variations with respect to initial conditions at survey III

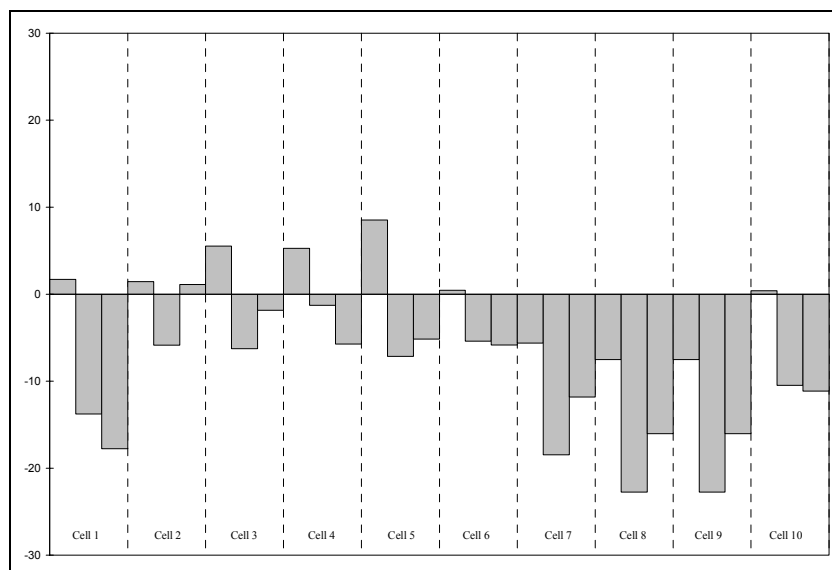


Figure 25: Shoreline variations with respect to initial conditions at survey IV

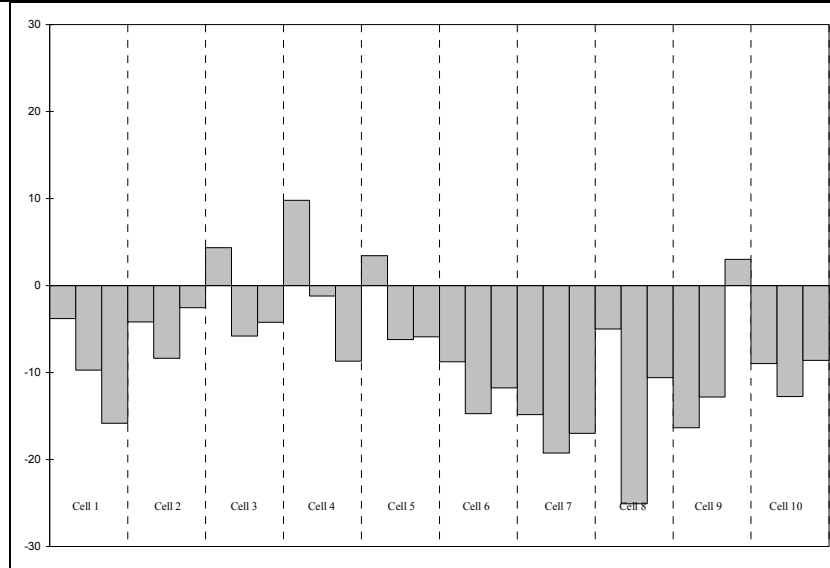


Figure 26: Shoreline variations with respect to initial conditions at survey V

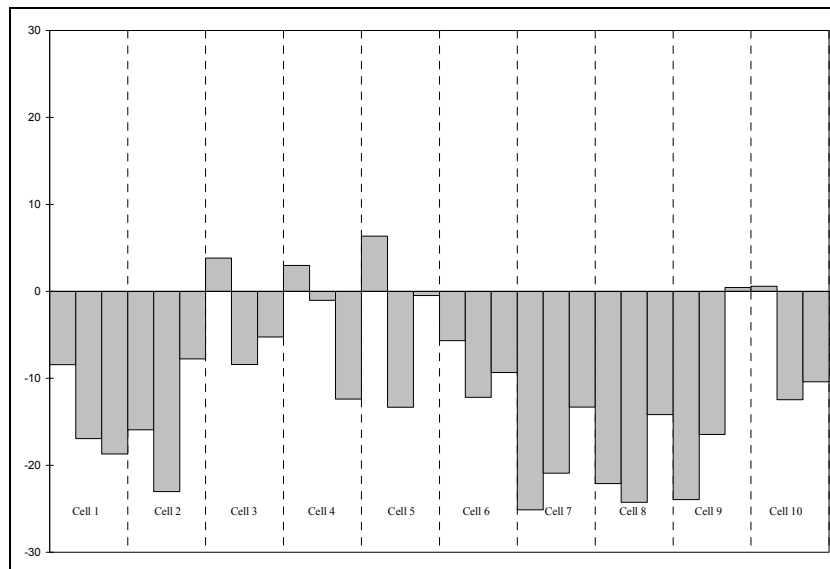


Figure 27: Shoreline variations with respect to initial conditions at survey VI

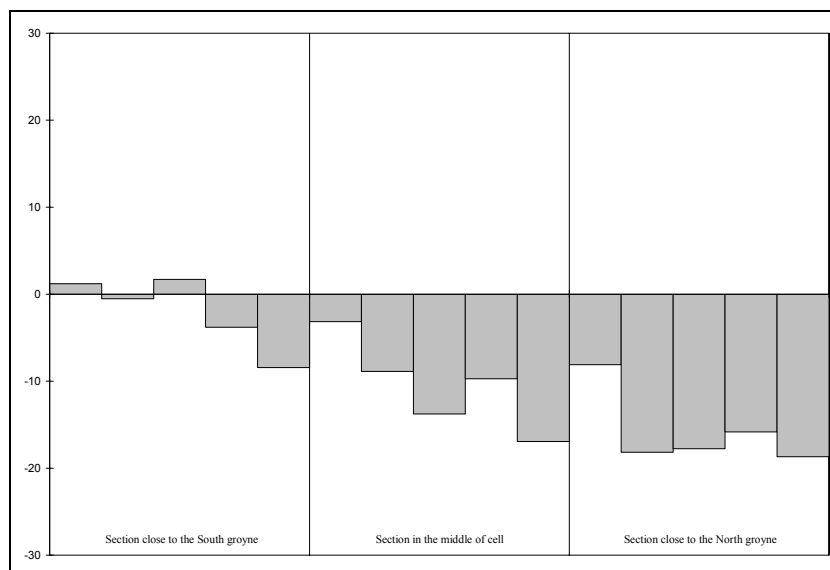


Figure 28: Shoreline variations with respect to initial conditions at cell 1 for all six surveys

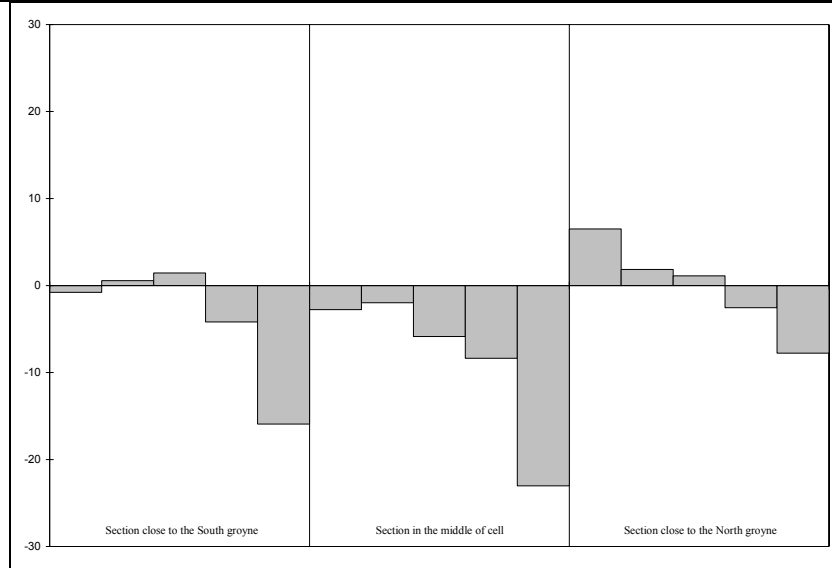


Figure 29: Shoreline variations with respect to initial conditions at cell 2 for all six surveys

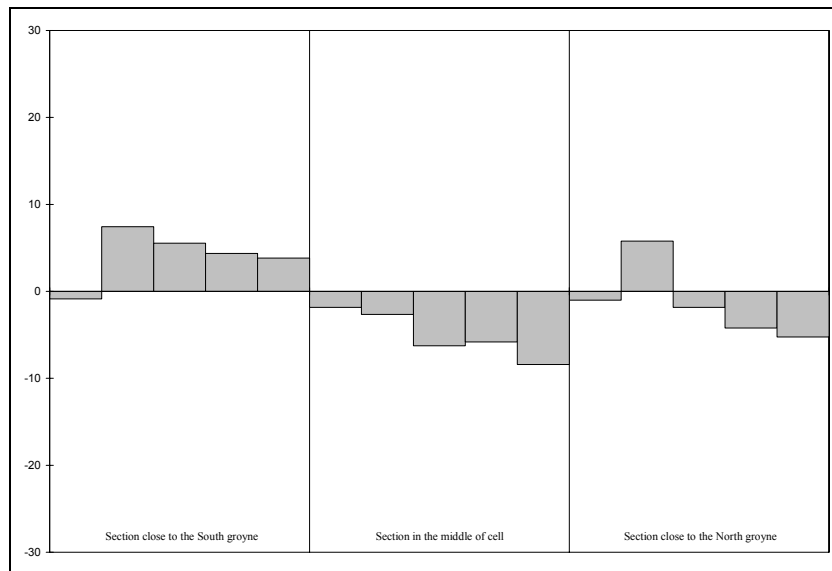


Figure 30: Shoreline variations with respect to initial conditions at cell 3 for all six surveys

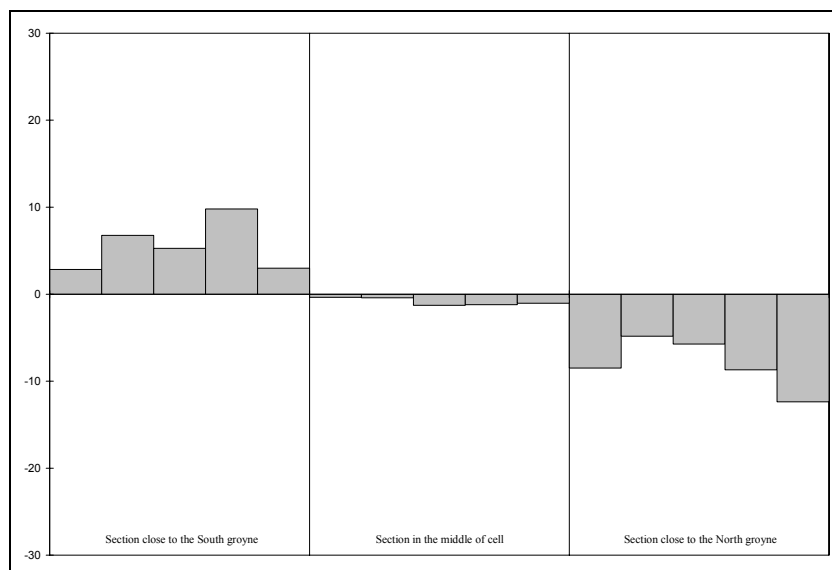


Figure 31: Shoreline variations with respect to initial conditions at cell 4 for all six surveys

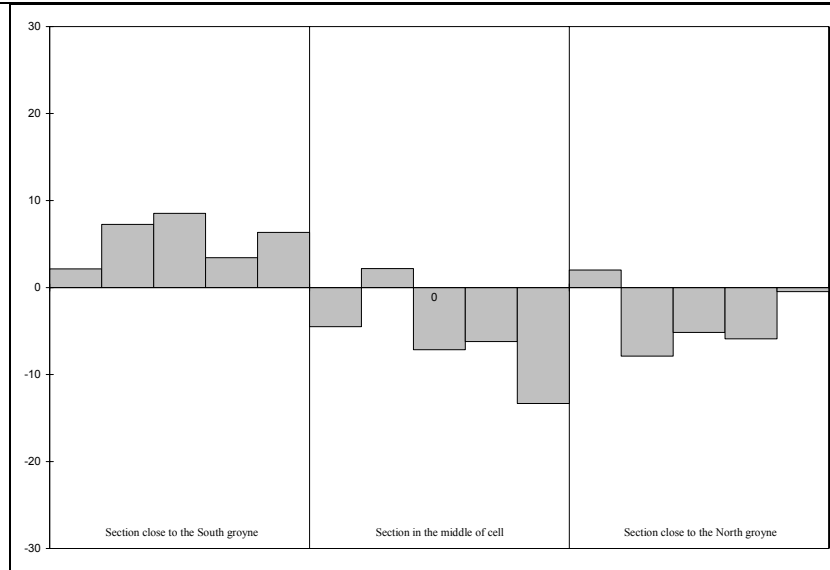


Figure 32: Shoreline variations with respect to initial conditions at cell 5 for all six surveys

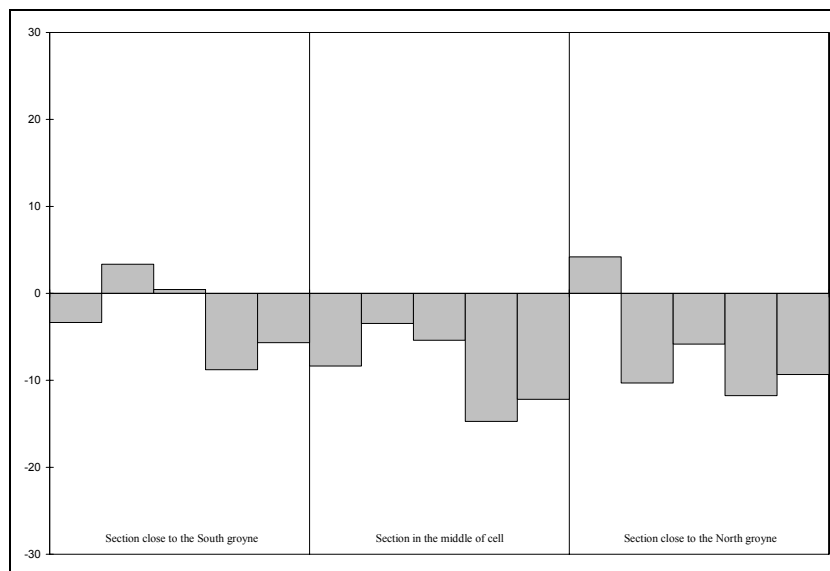


Figure 33: Shoreline variations with respect to initial conditions at cell 6 for all six surveys

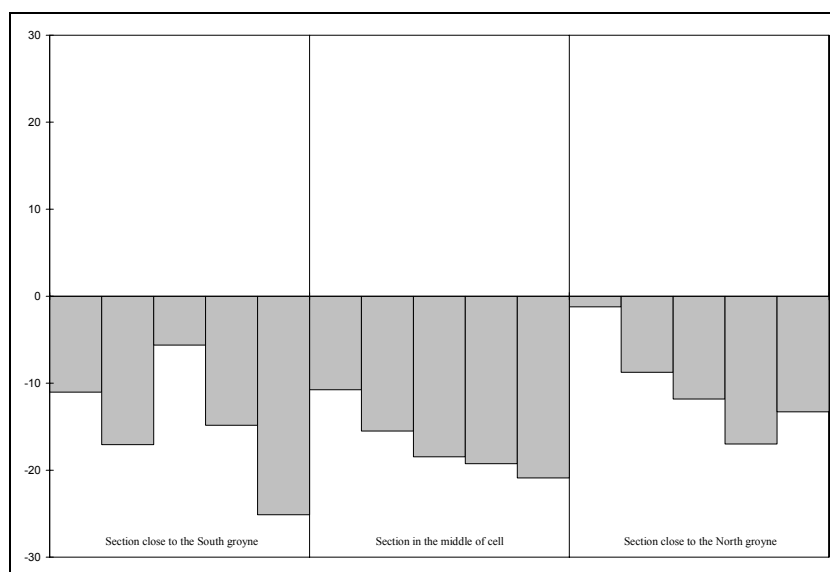


Figure 34: Shoreline variations with respect to initial conditions at cell 7 for all six surveys

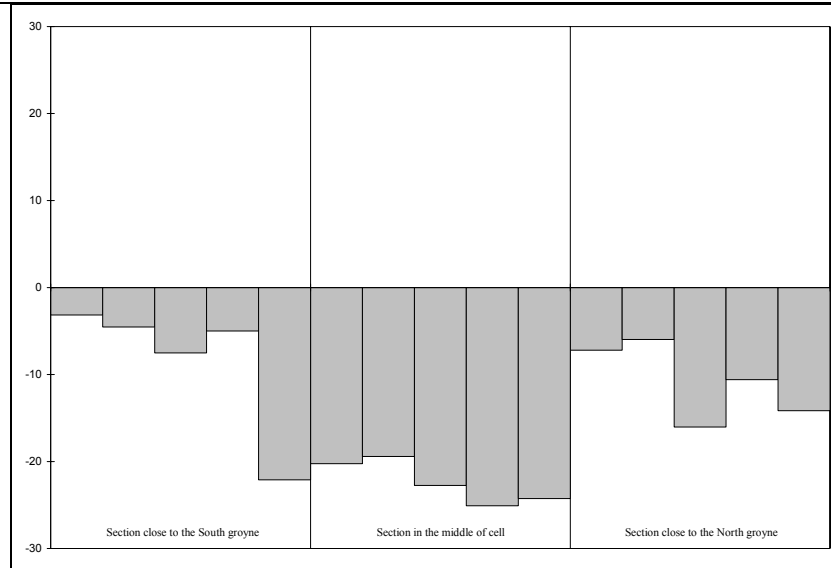


Figure 35: Shoreline variations with respect to initial conditions at cell 8 for all six surveys

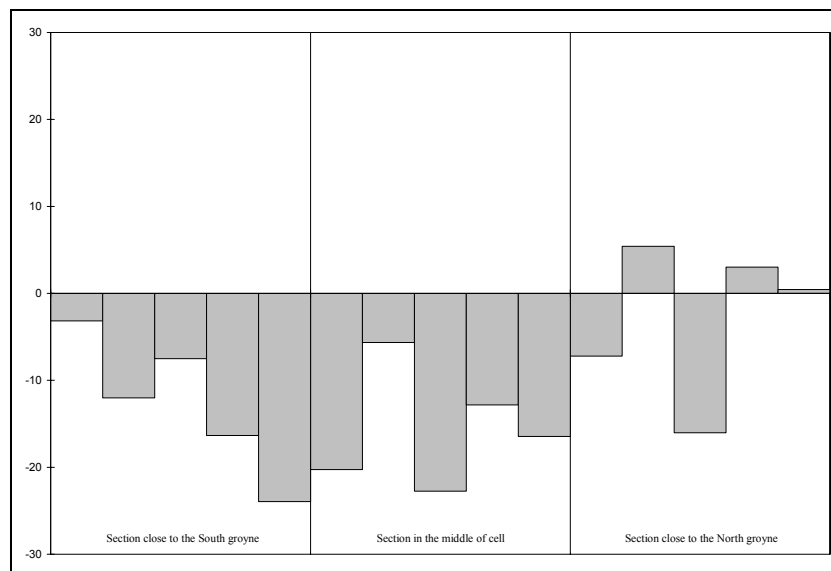


Figure 36: Shoreline variations with respect to initial conditions at cell 9 for all six surveys

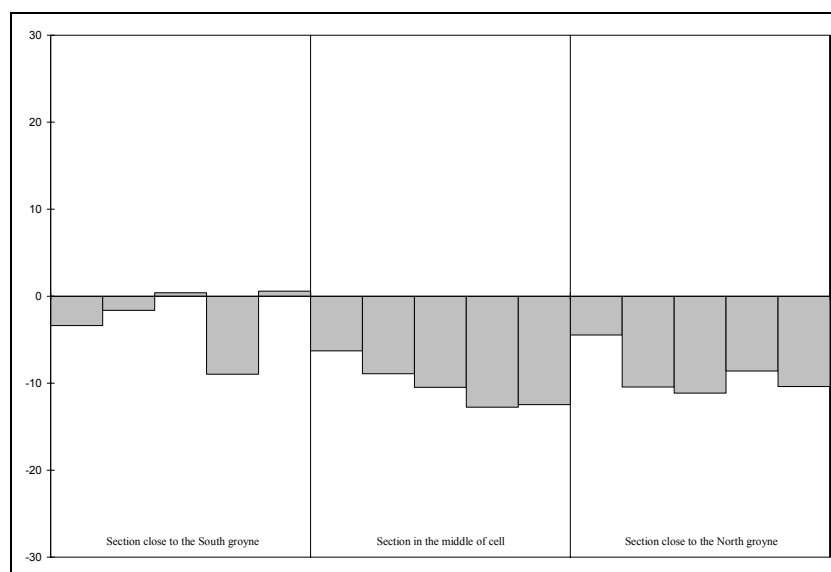


Figure 37: Shoreline variations with respect to initial conditions at cell 10 for all six surveys

In the graphs presented above it is possible to understand the spatial evolution of the shoreline position (fig. 23-24-25-26-27) along the ten cells at each survey. The first cells are more stable than the last. These graphs confirm the presence of reshaping phenomena in the youngest cells for which the shoreline presents large erosion with respect to the initial position.

The same results can be obtained regarding the temporal evolution of the shoreline position for each cell (fig. 28-29-30-31-32-33-34-35-36-37) and it is also possible to appreciate the plan shape of the shoreline for the last cells. For these ones, the initial plan shape of the shoreline is linear and about directed orthogonally to the groynes (as result of the nourishment operations) and the differential evolution on the three sections give an idea regarding this aspect.

For example, regarding cell 9 (fig. 36), for survey II carried on October 1997 (the first bar for each section) the shoreline takes the typical shape of pocket beach with a large erosion in the middle of the cell and smaller erosion close to the groynes. For survey III carried on July 1998 (the second bar for each section) the shoreline has a different behaviour: it is obliquely placed with erosion close to the South groyne and deposition close to the North one. Therefore it is possible to understand that the most severe waves come from South with respect to the orthogonal to the cell (see fig. 38 and fig. 22).

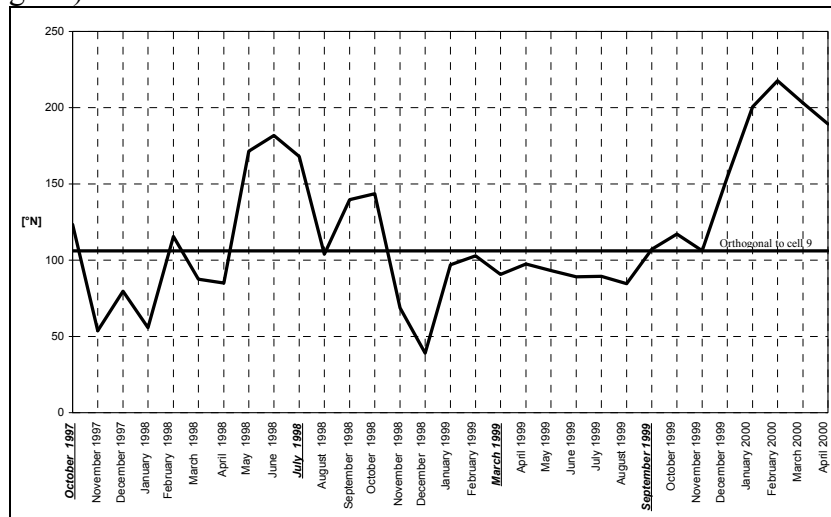


Figure 38: Wave direction distribution along time (mean month direction)

Similar comments can be done for the other surveys.

More information can be got up from the single section splitting up them in four regions (see fig. 39). A region (zone 1) near shoreline with a width of 100 m, a middle region (zone 2) begins at 100 m from section start to 60 m before the submerged breakwater crest, a third region (zone 3) from end of the middle one to the submerged breakwater crest and last region (zone 4) from submerged breakwater crest to the end of section.

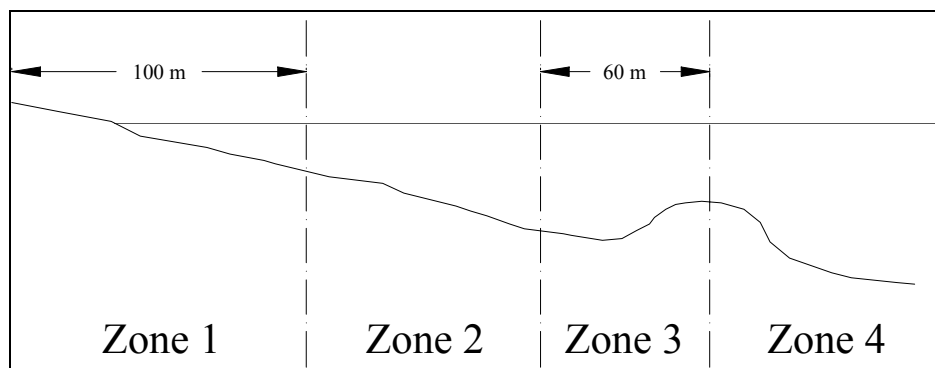


Figure 39: Sketch of the zones definition



By means of this zone definition it is possible to analyze the total area computation results for each region. For each section the total area was computed, but four areas was computed to observe the exchange of sand between different zones. Graphs of these areas for the cell 9 are presented in the following (fig. 40-41-42).

For the section close to the South groyne it is clearly observable that if there is a positive evolution of the total area, it is not true that there is a positive one for each region. For example, observing the graphs of the section in the middle of cell (fig. 41) it is clear for survey V that the zone 1 (the second bar) indicates negative evolution of the area whilst the total area evolution (first bar) is positive. For the other surveys of this section it is observable that the zone 1 always has a loss of sand that indicates the reshaping phenomena with transport of sand from beach to a zone far from the shoreline. In fact zone 2 (third bar) is always with positive evolution. Also, observing the zone 3 and zone 4 (fourth and fifth bars) it is possible to understand the transport of sand close to the submerged breakwater.

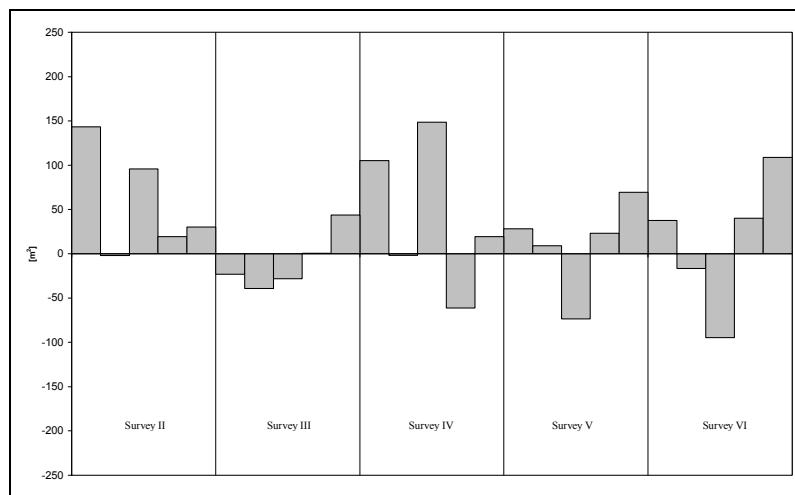


Figure 40: Areas evolution of the different zones for the section close to the South groyne with respect to the initial conditions

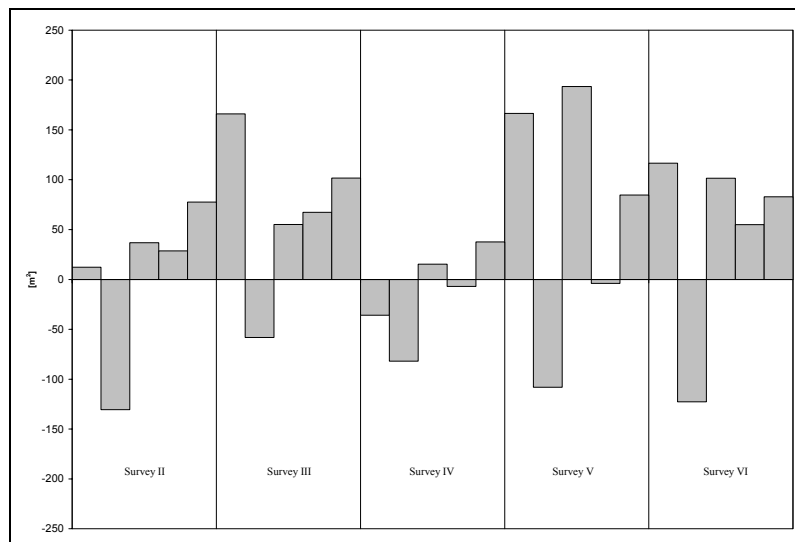


Figure 41: Areas evolution of the different zones for the section in the middle of cell 9 with respect to the initial conditions

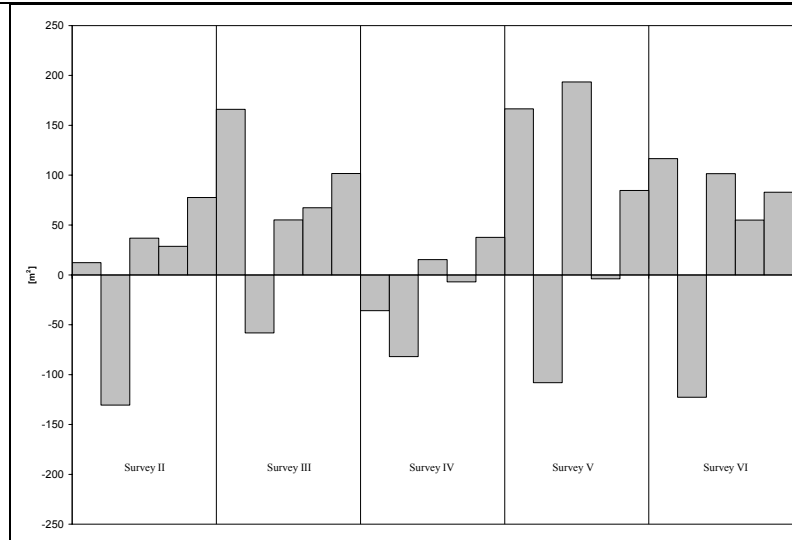


Figure 42: Areas evolution of the different zones for the section close to the North groyne with respect to the initial conditions

7. Conclusions and further work

At the end of this document it is important to underline that the computation presented let us know if there was a loss or gain of sand in the cells, but we cannot assert where the sand went in the loss case or where the sand came from in the gain case.

The situation of the system structures defence built at Lido of Pellestrina is good because the sand quantities were trapped in efficient manner: for the first cells (the South ones) the relative volumes percentage variations normalized with the cell nourishment volume is about 2% in three years, whilst for the last (the youngest ones) this variation are more important due to the reshaping phenomena (see tab. III: Volumes data). The project foresees a loss about 10% in ten years, so the results are acceptable.

Further studies will apply a one-line model to split the gain or loss of sand into longshore transport and transversal transport ratios. In this manner it will be possible to understand the displacement of the sand along the Lido of Pellestrina. Also in the future it will be possible to utilize the other cells surveys to understand not only the behaviour of the system structures defence in the first eleven cells but in the entire Lido.

In the following volume evolution graphs for each cell are presented.

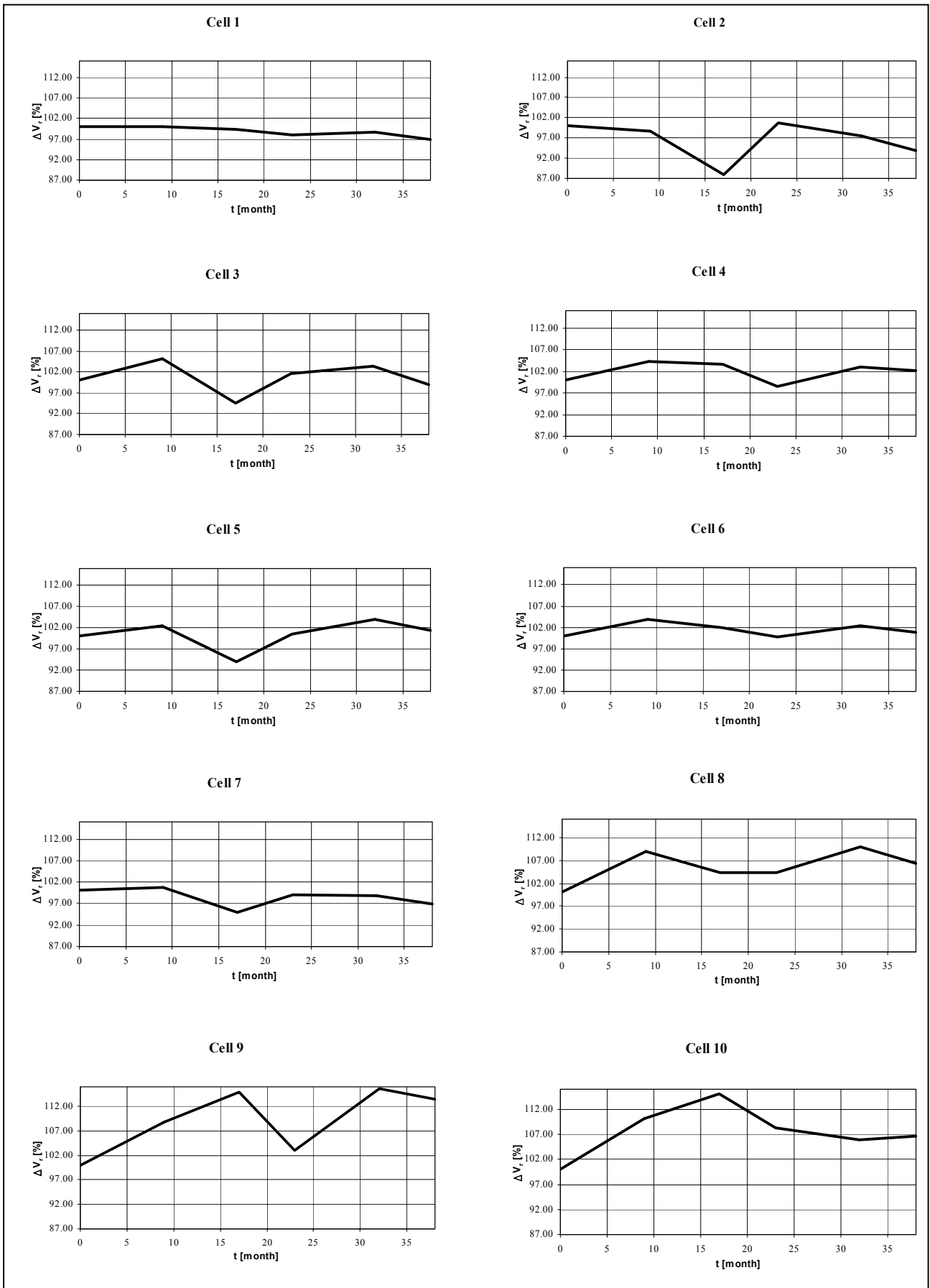


Figure 43: Volume evolution For each cell